INFECTION AND IMMUNITY, Sept. 2009, p. 3978–3991 Vol. 77, No. 9
0019-9567/09/$08.00+0 doi:10.1128/IAI.00616-09

Relevant Role of Fibronectin-Binding Proteins in *Staphylococcus aureus* Biofilm-Associated Foreign-Body Infections▽†

Marta Vergara-Irigaray,[1] Jaione Valle,[1] Nekane Merino,[1] Cristina Latasa,[1] Begoña García,[1] Igor Ruiz de los Mozos,[1] Cristina Solano,[1] Alejandro Toledo-Arana,[1] José R. Penadés,[2] and Iñigo Lasa[1]*

Laboratory of Microbial Biofilms, Instituto de Agrobiotecnología, Universidad Pública de Navarra-CSIC-Gobierno de Navarra, 31006 Pamplona, Spain,[1] and Centro de Investigación y Tecnología Animal, Instituto Valenciano de Investigaciones Agrarias (CITA-IVIA), Apdo 187, 12400 Segorbe, Castellón, Spain[2]

Received 31 May 2009/Returned for modification 15 June 2009/Accepted 24 June 2009

Staphylococcus aureus **can establish chronic infections on implanted medical devices due to its capacity to form biofilms. Analysis of the factors that assemble cells into a biofilm has revealed the occurrence of strains that produce either a polysaccharide intercellular adhesin/poly-*N*-acetylglucosamine (PIA/PNAG) exopolysaccharide- or a protein-dependent biofilm. Examination of the influence of matrix nature on the biofilm capacities of embedded bacteria has remained elusive, because a natural strain that readily converts between a polysaccharide- and a protein-based biofilm has not been studied. Here, we have investigated the clinical methicillin (meticillin)-resistant *Staphylococcus aureus* strain 132, which is able to alternate between a proteinaceous and an exopolysaccharidic biofilm matrix, depending on environmental conditions. Systematic disruption of each member of the LPXTG surface protein family identified fibronectin-binding proteins (FnBPs) as components of a proteinaceous biofilm formed in Trypticase soy broth-glucose, whereas a PIA/PNAG-dependent biofilm was produced under osmotic stress conditions. The induction of FnBP levels due to a spontaneous *agr* deficiency present in strain 132 and the activation of a LexA-dependent SOS response or FnBP overexpression from a multicopy plasmid enhanced biofilm development, suggesting a direct relationship between the FnBP levels and the strength of the multicellular phenotype. Scanning electron microscopy revealed that cells growing in the FnBP-mediated biofilm formed highly dense aggregates without any detectable extracellular matrix, whereas cells in a PIA/PNAG-dependent biofilm were embedded in an abundant extracellular material. Finally, studies of the contribution of each type of biofilm matrix to subcutaneous catheter colonization revealed that an FnBP mutant displayed a significantly lower capacity to develop biofilm on implanted catheters than the isogenic PIA/PNAG-deficient mutant.**

Staphylococcus aureus is a human pathogen that causes both nosocomial and community-acquired infections that can range from minor skin infections to life-threatening illnesses such as endocarditis, osteomyelitis, or toxic shock syndrome. The emergence of highly virulent strains, resistant to many antibiotics, such as methicillin (meticillin)-resistant *S. aureus* (MRSA) is of considerable concern worldwide (21, 24). In addition, patients with indwelling medical devices can easily develop staphylococcal infections, due to the ability of *S. aureus* to colonize the implant surface as a biofilm. Inside the biofilm, bacteria are enclosed in a self-produced, hydrated polymeric matrix that confers increased resistance to desiccation and increased tolerance to antimicrobial agents and the host immune response by mechanisms that are still somewhat unclear.

The biofilm matrix is a complex mixture of macromolecules, including exopolysaccharides, proteins, and DNA. The main exopolysaccharide of the *S. aureus* biofilm matrix is a polymer of poly-*N*-acetyl-β-(1-6)-glucosamine, termed polysaccharide intercellular adhesin (PIA) or poly-*N*-acetylglucosamine (PNAG), whose synthesis depends on the enzymes encoded by the *icaADBC* operon (10, 19, 32). The presence of PIA/PNAG exopolysaccharide is not essential for biofilm development, since several studies have uncovered the existence of *S. aureus* isolates able to produce alternative biofilm matrixes (6, 9, 11, 14, 28, 33, 36, 45, 46, 49). When this occurs, it appears that proteins usually take the responsibility for mediating cell-to-cell interactions and multicellular behavior. Interestingly, protein-mediated biofilm formation capacity seems to be particularly frequent among the highly virulent MRSA isolates, emphasizing the importance of this type of biofilm structure (14, 37).

The first example of a surface protein able to induce biofilm development was Bap. Bap is a large cell wall-associated protein able to mediate primary attachment to abiotic surfaces and intercellular adhesion (11). So far, the presence of Bap has only been described in mastitis-derived staphylococci (11, 50). The second example was SasG, a protein involved in adhesion to desquamated nasal epithelial cells, whose overexpression induces the formation of peritrichous fibrils of various densities on the cell wall and biofilm development (9, 27). More recently, two independent research groups have described a novel *S. aureus* biofilm phenotype mediated by the fibronectin-binding proteins, FnBPA and FnBPB (36, 46). Finally, we have very recently shown that increased accumulation of protein A

* Corresponding author. Mailing address: Instituto de Agrobiotecnología, Universidad Pública de Navarra, Pamplona-31006, Spain. Phone: 34 948 168007. Fax: 34 948 232191. E-mail: ilasa@unavarra.es.

† Supplemental material for this article may be found at http://iai.asm.org/.

▽ Published ahead of print on 6 July 2009.

in *agr* mutants, and more significantly in double *agr-arlRS* mutants, contributes to biofilm formation capacity (33, 49).

All genes encoding exopolysaccharidic and proteinaceous factors involved in the biofilm formation process, with the exception of *bap*, are widely distributed among *S. aureus* isolates. However, as stated above, not all of these compounds simultaneously take part in a particular biofilm, suggesting that *S. aureus* regulates the production of different types of matrixes depending on the environmental conditions. Thus, biofilm matrix composition might simply depend on the availability of the nutrients necessary to provide energy and biosynthetic intermediates for the synthesis of the matrix macromolecules. As a consequence of the environment encountered, every synthesized matrix would confer specific capacities to embedded bacteria. In this respect, the properties that each type of biofilm matrix bestow on the bacterial community remain unknown, because an *S. aureus* strain that readily converts between polysaccharidic and protein-based biofilms has not been investigated.

In this study, we have identified and analyzed a MRSA *S. aureus* isolate able to modulate the composition of the biofilm matrix, producing either a PIA/PNAG- or FnBP-mediated biofilm, depending on the environmental conditions. Interestingly, we have demonstrated that induction of FnBP levels due to a spontaneous *agr* mutation, as well as activation of the SOS response in a LexA-dependent manner, promotes FnBP biofilms. In addition, the analysis of the significance of each biofilm matrix in a murine foreign-body infection model revealed that in the case of strain 132, FnBPs played a more relevant role than PIA/PNAG during the in vivo colonization of catheters.

MATERIALS AND METHODS

Bacterial strains and growth conditions. The most relevant bacterial strains and plasmids used in this study are listed in Table 1. The 63 *ica*-positive clinical isolates tested for their capacity to form biofilms are listed in Table S1 in the supplemental material. They were isolated at the Microbiology Department of the Clínica Universitaria de Navarra (Pamplona, Spain) and at the Centre National de Référence des Staphylocoques (Hôpital Edouard Herriot, Lyon, France).

Escherichia coli XL1-Blue cells were grown in Luria-Bertani (LB) broth or on LB agar (Pronadisa, Spain). Staphylococcal strains were cultured on Trypticase soy agar (TSA), on Congo red agar, or in Trypticase soy broth (TSB) supplemented with 0.25% glucose (TSB-gluc) or 3% NaCl (TSB-NaCl). Congo red agar was prepared as follows: 30 g/liter of Trypticase soy (Pronadisa), 15 g/liter of agar (Pronadisa), 0.8 g/liter of Congo red stain (Sigma), and 20 g/liter of sucrose. The Congo red stain and the sucrose solution were autoclaved separately (121°C for 20 min and 115°C for 15 min, respectively). For assessment of the hemolysin activity induced by RNAIII, sheep blood agar plates were used (Biomérieux).

Media were supplemented with appropriate antibiotics at the following concentrations: erythromycin (*erm*) at 1.5 μg ml^{-1} or 10 μg ml^{-1}; ampicillin at 100 μg ml^{-1}; chloramphenicol at 5 μg ml^{-1}; and tetracycline (*tet*) at 3 μg ml^{-1} or 125 ng ml^{-1}.

DNA manipulations. DNA plasmids were isolated from *E. coli* using a Bio-Rad plasmid miniprep kit (Bio-Rad Laboratories, Inc.) according to the manufacturer's protocol. Plasmids were transformed into staphylococci by electroporation, using a previously described protocol (11).

Restriction enzymes were purchased from New England Biolabs and used according to the manufacturer's instructions. DNA polymerase was purchased from Biotools. Oligonucleotides were obtained from Thermo Electron Corporation (see Table S2 in the supplemental material).

For detection of the *icaADBC* operon in *S. aureus* strains, the *icaA* and *icaC* genes were amplified by PCR using primers *icaA-1*/*icaA-2* and *icaC-1*/*icaC-2*, respectively, (see Table S2 in the supplemental material).

For Southern hybridization, chromosomal DNA was purified, digested, and analyzed by agarose gel electrophoresis. DNA fragments were transferred by alkaline capillary blotting onto nylon membranes (GE Healthcare) using standard methods (3). Labeling of the probe and DNA hybridization were performed according to the protocol supplied with the DIG DNA labeling and detection kit (Roche).

The substitution of glutamate for glycine at the Ala-Gly cleavage site of LexA was performed as previously described (52).

The genome of *S. aureus* strain 132 was sequenced using the 454 pyrosequencing strategy on a GS FLX sequencer (LifeSequencing SL, Valencia, Spain) and resulted in the generation of 66 Mb of sequences. The GS FLX reads were assembled into 44 large contigs longer than 1,000 bp (GenBank accession number ACOT01000000).

Allelic exchange of chromosomal genes. To generate deletion mutants, we amplified by PCR two fragments of 500 bp that flanked the left (primers A and B) and right (primers C and D) sequences of the genes targeted for deletion (see Table S2 in the supplemental material). The PCR products were purified and cloned separately in a pGEM-T Easy vector (Promega). Fragments were then fused by ligation into the shuttle plasmid pMAD, and the resulting plasmids were transformed into *S. aureus* by electroporation. pMAD contains a temperature-sensitive origin of replication and an erythromycin resistance gene (1). Homologous recombination experiments were performed as previously described (53). Erythromycin-sensitive white colonies, which no longer contained the pMAD plasmid, were tested by PCR using primers E and F (see Table S2 in the supplemental material). Deletion mutants of *spa*, *sdrD*, *agr*, and *ica* were constructed as previously described (33, 49, 53).

Construction of insertional mutations. For disruption of the *clfA*, *clfB*, *sdrC*, *sasA*, *sasD*, *sasE*, *sasF*, *sasH*, *sasI*, *sasJ*, SA0927, and SA1888 genes in strain 132 (Table 1), a PCR fragment within the A regions of the different genes was amplified using the respective primers 1 and 2 (see Table S2 in the supplemental material) and cloned in a pGEM-T Easy vector (Promega). The corresponding fragments were then cloned into the shuttle vector pMAD, and the resulting plasmids were transformed into *S. aureus* by electroporation. The plasmids were integrated into the chromosome through homologous recombination at a nonpermissive temperature (44°C). The disruption of the respective genes was confirmed by PCR using the pMAD-1 primer and the corresponding primer 3 external to each construction (see Table S2 in the supplemental material).

The *srtA*::*ermC* mutation was transduced from *S. aureus* Newman SKM3 (31) into *S. aureus* strain 132 using phage 85α. The disruption of the gene was confirmed by PCR using primers *srtA-3* and *srtA-4* (see Table S2 in the supplemental material).

The *fnbA*::*tet* and *fnbB*::*erm* mutations were transduced from *S. aureus* DU 5883 (17) into *S. aureus* strain 132 and the 132 Δ*ica* mutant using phage 85α. The disruption of the respective genes was confirmed by Southern blotting (data not shown).

The *ica*::*tet* mutation was transduced into *S. aureus* strain 132 from *S. aureus* SA113 Δ*ica*, which contains a tetracycline resistance cassette that replaces *ica* genes (10) using phage 85α. All transductions were performed as described previously (34).

Complementation experiments. For complementation experiments, the multicopy plasmids pFNBA4 and pFNBB4 (17) that carry, respectively, the wild-type *fnbA* and *fnbB* genes of *S. aureus* 8325-4 were used. The empty plasmid pALC2073 was used as a control (Table 1). For complementation of *agr* deficiency, RNAIII was amplified by PCR using primers RNA III-1 and -2 (see Table S2 in the supplemental material) and chromosomal DNA from strain ISP479c as template. The PCR product was purified and cloned at the EcoRI site of the pALC2073 plasmid, downstream of the tetracycline-inducible promoter. Correct orientation of the insert was confirmed by restriction mapping. Expression was induced with 125 ng ml^{-1} of tetracycline.

Biofilm formation and detachment assays. The biofilm formation assays in microtiter wells were performed as previously described (18). Sterile 96-well polystyrene microtiter plates from the same manufacturer (Iwaki) were used throughout the study. Each assay was performed in triplicate and repeated at least three times. Crystal violet-stained cells were quantified by solubilizing the dye with 200 μl of ethanol-acetone (80:20, vol/vol) and determining the optical density at 595 nm (OD_{595}).

For adherence assays in a glass tube, a single colony was transferred to 5 ml of TSB-gluc in a 15-ml tube and incubated at 37°C in an orbital shaker (250 rpm) for 12 h.

The colony morphology of *S. aureus* strains was analyzed using Congo red agar plates. Briefly, 5 μl of overnight cultures of *S. aureus* strains were spotted onto Congo red agar plates and incubated at 37°C for 24 h.

To test whether the activation of the SOS response induced biofilm formation,

TABLE 1. Most relevant strains and plasmids used in this study

Strain or plasmid	Relevant characteristic(s)	Source
Strains		
S. aureus		
132	MRSA clinical strain; biofilm positive	This study
15981	Clinical strain	53
115	Clinical strain	This study
8061	Clinical strain	This study
G-6478	MRSA clinical strain	This study
10833	Clumping factor-positive variant of Newman D2C	10
ISP479c	ISP479 cured of plasmid	38
RN4220	A mutant of *S. aureus* strain 8325-4 that accepts foreign DNA	35
132 Δ*ica*	132 with deletion of the *icaADBC* operon	This study
132 *ica*	132 *ica*::*tet*	This study
132 Δ*agr*	132 with deletion of the *agrBDCA* operon	This study
132 Δ*spa*	132 with deletion of the *spa* gene	This study
132 *clfA*	132 *clfA*::pMAD	This study
132 *clfB*	132 *clfB*::pMAD	This study
132 Δ*fnbA*	132 with deletion of the *fnbA* gene	This study
132 Δ*fnbB*	132 with deletion of the *fnbB* gene	This study
132 Δ*fnbAB*	132 with deletion of the *fnbA* and *fnbB* genes	This study
132 Δ*ica* Δ*fnbA*	132 with deletion of the *icaADBC* and *fnbA* genes	This study
132 Δ*ica* Δ*fnbB*	132 with deletion of the *icaADBC* and *fnbB* genes	This study
132 Δ*ica* Δ*fnbAB*	132 with deletion of the *icaADBC*, *fnbA*, and *fnbB* genes	This study
132 *fnbAB*	132 *fnbA*::*tet fnbB*::*erm*	This study
132 Δ*ica fnbAB*	132 *fnbA*::*tet fnbB*::*erm* with deletion of the *icaADBC* genes	This study
132 *sdrC*	132 *sdrC*::pMAD	This study
132 Δ*sdrD*	132 with deletion of the *sdrD* gene	This study
132 Δ*sdrE*	132 with deletion of the *sdrE* gene	This study
132 *sasA*	132 *sasA*::pMAD	This study
132 Δ*fmtB* (Δ*sasB*)	132 with deletion of the *fmtB* gene	This study
132 Δ*sasC*	132 with deletion of the *sasC* gene	This study
132 *sasD*	132 *sasD*::pMAD	This study
132 *sasE*	132 *sasE*::pMAD	This study
132 *sasF*	132 *sasF*::pMAD	This study
132 Δ*sasG*	132 with deletion of the *sasG* gene	This study
132 *sasH*	132 *sasH*::pMAD	This study
132 *sasI*	132 *sasI*::pMAD	This study
132 *sasJ*	132 *sasJ*::pMAD	This study
132 SA0927	132 SA0927::pMAD	This study
132 SA1888	132 SA1888::pMAD	This study
132 *srtA*	132 *srtA*::*erm*	This study
132 *lexA*	132 LexA(G94E)	This study
132 Δ*fnbAB* pFNBA4	132 Δ*fnbAB* complemented with the *fnbA* gene	This study
132 Δ*fnbAB* pFNBB4	132 Δ*fnbAB* complemented with the *fnbB* gene	This study
132 Δ*fnbAB* pALC2073	132 Δ*fnbAB* transformed with the pALC2073 plasmid	This study
132 Δ*ica* Δ*fnbAB* pFNBA4	132 Δ*ica* Δ*fnbAB* complemented with the *fnbA* gene	This study
132 Δ*ica* Δ*fnbAB* pFNBB4	132 Δ*ica* Δ*fnbAB* complemented with the *fnbB* gene	This study
132 Δ*ica* Δ*fnbAB* pALC2073	132 Δ*ica* Δ*fnbAB* transformed with the pALC2073 plasmid	This study
132 pFNBA4	132 complemented with the *fnbA* gene	This study
132 pFNBB4	132 complemented with the *fnbB* gene	This study
132 pALC2073	132 transformed with the pALC2073 plasmid	This study
132 pALC2073RNAIII	132 transformed with the pALC2073RNAIII plasmid	This study
RN4220 pFNBA4	RN4220 complemented with the *fnbA* gene	This study
RN4220 pFNBB4	RN4220 complemented with the *fnbB* gene	This study
RN4220 pALC2073	RN4220 transformed with the pALC2073 plasmid	This study
G-6478 pFNBA4	G-6478 complemented with the *fnbA* gene	This study
G-6478 pFNBB4	G-6478 complemented with the *fnbB* gene	This study
G-6478 pALC2073	G-6478 transformed with the pALC2073 plasmid	This study
10833 pFNBA4	10833 complemented with the *fnbA* gene	This study
10833 pFNBB4	10833 complemented with the *fnbB* gene	This study
10833 pALC2073	10833 transformed with pALC2073 the plasmid	This study
E. coli		
XL1Blue	Used for cloning assays	
Plasmids		
pGEM-T	Used for cloning assays	Promega
pMAD	*E. coli-S. aureus* shuttle vector with a thermosensitive origin of replication for gram-positive bacteria	1
pFNBA4	Vector for *fnbA* complementation experiments	17
pFNBB4	Vector for *fnbB* complementation experiments	17
pALC2073	*E. coli-S. aureus* shuttle vector with a tetracycline-inducible promoter.	4
pALC2073RNAIII	pALC2073 with RNAIII cloned into the EcoRI site	This study

0.05 μg/ml of mitomycin C (Sigma) was added to the growth media at the time of inoculation.

To study biofilm formation in the presence of RNAIII, RNAIII expression by pALC2073RNAIII was induced with 125 ng ml^{-1} of tetracycline at the time of inoculation.

To analyze biofilm formation under flow conditions, we used 60-ml microfermenters (Pasteur Institute, Laboratory of Fermentation) with a continuous 40-ml h^{-1} flow of medium and constant aeration with sterile compressed air (0.3 bar). Submerged Pyrex slides served as growth substratum. Approximately 10^8 bacteria from an overnight culture of each strain grown in the appropriate medium were used to inoculate the microfermenters that were then kept at 37°C for 24 h. Biofilm development was recorded with a Nikon Coolpix 950 digital camera. To

quantify the biofilm formed, bacteria adhered to the Pyrex slides were resuspended in 20 ml of TSB-gluc. The OD_{650} of the suspensions was then determined.

Biofilm detachment assays with sodium metaperiodate (Scharlau) and proteinase K (Sigma) were carried out as previously described (22).

Scanning microscopy. Scanning electron microscopy was performed on biofilms grown in microfermenters on Thermanox slides (Nalgene Nunc International) fixed on the internal removable glass slides, as described by Prigent-Combaret et al. (39) at the Laboratoire de Biologie Cellulaire et Microscopie Electronique, UFR Médecine (Tours, France).

PIA/PNAG detection. Cell surface PIA/PNAG exopolysaccharide levels were detected as previously described (10). Overnight cultures of the strains tested were diluted 1:40 in the appropriate medium, and 2 ml of this cell suspension was used to inoculate sterile 24-well polystyrene microtiter plates (Sarstedt). After 24 h of static incubation at 37°C, the same number of cells of each strain was resuspended in 50 μl of 0.5 M EDTA (pH 8.0). Then, cells were incubated for 5 min at 100°C and centrifuged to the pellet. Each supernatant (40 μl) was incubated with 10 μl of proteinase K (20 mg/ml; Sigma) for 30 min at 37°C. After the addition of 10 μl of Tris-buffered saline (20 mM Tris-HCl, 150 mM NaCl [pH 7.4]) containing 0.01% bromophenol blue, 5 μl was spotted on a nitrocellulose filter using a Bio-Dot microfiltration apparatus (Bio-Rad), blocked overnight with 5% skimmed milk in phosphate-buffered saline (PBS) with 0.1% Tween 20, and incubated for 2 h with rabbit antibodies raised to *S. aureus* deacetylated PNAG conjugated to diphtheria toxoid diluted at 1:10,000 (30). Bound antibodies were detected with peroxidase-conjugated goat anti-rabbit immunoglobulin G antibodies (Jackson ImmunoResearch Laboratories, Inc., Westgrove, PA), diluted 1:10,000, and an Amersham ECL Western blotting system.

Real-time quantitative PCR. To study the transcription of *icaC* and *fnbB* in TSB-gluc and TSB-NaCl media, an overnight culture of strain 132 was diluted (1:100) in the appropriate medium and grown to exponential phase (OD_{600} = 0.6). Total *S. aureus* RNA was isolated using a Fast RNA-Blue kit (MP Biomedicals, LLC) according to the manufacturer's instructions. In order to minimize variability, nine independent RNAs were purified from each strain and divided into three pools. RNAs were then subjected to DNase (Ambion) treatment for 20 min at 37°C. After inactivation of the enzyme, and to verify the absence of genomic DNA, the RNAs were reverse transcribed in the presence and absence of reverse transcriptase (RT) (SuperScript III RT; Invitrogen). All preparations were purified using Qiagen columns (QIAquick PCR purification kit). To measure expression, *icaC* transcripts were amplified using primers *icaC2*-SG-5 and *icaC2*-SG-3 and SYBR GreenER SuperMix (Invitrogen), and *fnbB* transcripts were amplified using primers *fnbB*-FW and *fnbB*-RV (see Table S2 in the supplemental material).

An ABI PRISM model 9700HT (Applied Biosystems) instrument was used to monitor the real-time quantitative PCR. The *gyrB* transcripts that were constitutively expressed were amplified as endogenous controls by using primers *gyrB*-SG-5 and *gyrB*-SG-3 (see Table S2 in the supplemental material). To monitor the specificity, final PCR products were analyzed by melting curves and electrophoresis. Only samples with no amplification of the minus RT aliquots were considered in the study. The amount of *icaC* and *fnbB* transcripts was expressed as the *n*-fold difference relative to the control gene ($2^{-\Delta Ct}$, where ΔCt represents the difference in threshold cycles between the target and control genes).

Western ligand affinity blotting. For detection of the level of FnBPs after induction of the SOS response, an overnight culture of strain 132 was diluted 1:50 in TSB-gluc medium supplemented with increasing mitomycin C concentrations (0.005, 0.01, 0.02, 0.04, and 0.06 μg/ml) and grown for 4 h, at 37°C, without shaking. The same number of cells of each strain was collected, and surface-associated protein extracts were prepared as previously described (2). For detection of the level of FnBPs after RNAIII induction, an overnight culture of strain 132 carrying pALC2073RNAIII was diluted 1:50 in TSB-gluc medium supplemented with 125 ng ml^{-1} of tetracycline, and 2 ml of this cell suspension was used to inoculate sterile 24-well polystyrene microtiter plates (Sarstedt). After 24 h of static incubation at 37°C, the same number of cells of each strain was collected, and surface-associated protein extracts were prepared as previously described (2).

Electrophoretic separation of cell wall-associated protein preparations was carried out by sodium dodecyl sulfate-polyacrylamide gel electrophoresis (SDS-PAGE). The acrylamide concentration was 8% in the resolving gel and 4% in the stacking gel. FnBPs were detected by Western ligand affinity blotting by incubation for 1 h with biotinylated human fibronectin (50 μg/ml) in PBS containing 0.1% Tween 20 (PBST). An EZ-Link sulfo-*N*-hydroxysuccinimide-LC biotinylation kit (Pierce) was used to biotinylate human fibronectin (Sigma). After washing with PBST, membranes were incubated for 1 h with streptavidin-peroxidase conjugate (Roche; 1:3,000 dilution). Finally, membranes were developed with the ECL Western blotting system. The strain 132 Δ*fnbAB* double mutant was used as an internal negative control.

Coinfection experiments. Prior to coinfection assays, a competition experiment was performed. The same number of bacteria coming from an overnight culture of each strain was used to inoculate 5 ml of TSB-gluc. After having grown together overnight, 100 μl of an optimal dilution were plated on TSA and TSA *tet*, in triplicate, in order to estimate plate counts corresponding to each strain.

To examine the in vivo interaction of *fnbAB* mutants with abiotic surfaces, the murine model of catheter-associated biofilm formation described by Beenken et al. was used with some modifications (6). Briefly, a total of 66 male Swiss mice were anesthetized with ketamine (100 mg/kg) and xylazine (10 mg/kg). Polyurethane catheters (15 mm; B. Braun Medical, Bethlehem, PA) were inserted and coinfected by injection of 200 μl of a 10^8 CFU/ml mixture containing the same quantity of either strain 132 and 132 *fnbAB*, strain 132 and 132 Δ*ica fnbAB*, or strain 132 and 132 *ica*. The skin of each mouse was cleansed with alcohol prior to surgery, and as a control of the procedure, six mice were infected with sterile PBS. Mice were euthanized at 3 or 7 days postinfection, and groups of 10 mice were used for each comparison. The catheters were removed aseptically, washed, and placed in 1 ml of sterile PBS. Catheters were then washed internally with the aid of a sterile syringe and sonicated to remove adherent bacteria. The number and identity of recovered bacteria was determined by plate count on TSA supplemented with and without tetracycline at 3 μg ml^{-1}. Competitive indexes were calculated by dividing the number of *tet*-sensitive CFU by the number of *tet*-resistant CFU.

Statistical analysis. Statistical analyses were performed with the GraphPad Prism program. *P* values assessing the significance of the difference from 1 of the competition indexes were calculated using the Wilcoxon's test. Data corresponding to gene expression were compared using the Mann-Whitney test. Differences were considered statistically significant when $P < 0.05$. In the biofilm quantification assays, microtiter plate data represent the means of at least nine measures from three independent experiments.

Nucleotide sequence accession number. The 44 large contigs sequenced in this study have been deposited in the GenBank database under accession number ACOT01000000.

RESULTS

Selection of an *S. aureus* isolate able to develop PIA/PNAG-dependent and -independent biofilms. With the aim of selecting a natural *S. aureus* isolate able to switch between the production of a polysaccharidic and a proteinaceous biofilm matrix depending on the environmental conditions, we first analyzed both the capacity to form a biofilm on polystyrene microtiter plates and the capacity to produce PIA/PNAG in TSB-gluc in a collection of 63 *ica*-positive *S. aureus* clinical isolates (see Table S1 in the supplemental material). The strains were classified into four groups: (i) biofilm positive-PIA/PNAG positive (16%); (ii) biofilm negative-PIA/PNAG positive (36%); (iii) biofilm positive-PIA/PNAG negative (19%); and (iv) biofilm negative-PIA/PNAG negative (29%). Figure 1A shows the biofilm formation and PIA/PNAG production of one representative strain from each group. Then, we focused on group III, which contained strains that are capable of forming a biofilm independently of PIA/PNAG synthesis under TSB-gluc growing conditions but are perhaps able to synthesize PIA/PNAG under conditions known to induce its synthesis (3% NaCl and subinhibitory concentrations of antibiotics) (37, 41, 42). Using this approach, we selected one isolate (MRSA strain 132) that formed a biofilm and produced detectable levels of PIA/PNAG when NaCl (3%) was added to the medium (Fig. 1B). To verify that PIA/PNAG was actually required for biofilm formation under TSB-NaCl and not TSB-gluc conditions, we generated a strain 132 Δ*icaADBC* deletion mutant and tested its biofilm formation capacity. The results confirmed that *ica* deletion had no impact on the capacity of MRSA strain 132 to produce a biofilm in TSB-gluc, whereas it

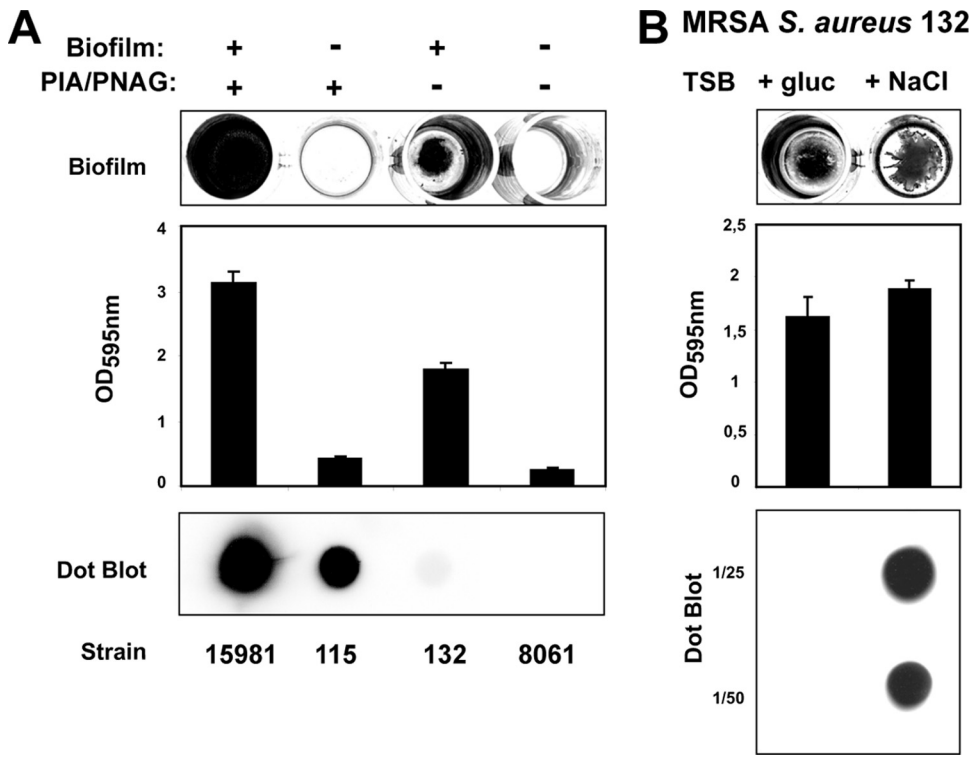

FIG. 1. Selection of the *S. aureus* MRSA strain 132. (A) Summary of the classification of 63 *ica*-positive *S. aureus* isolates according to their capacities to form biofilm and synthesize PIA/PNAG in TSB-gluc medium. Biofilm formation capacity on polystyrene microtiter plates after 24 h hours of growth at 37°C in TSB-gluc medium, quantification of the biofilm formed, and dot blot analysis of the PIA/PNAG produced by one representative *S. aureus* isolate of each group are shown (15981, 115, 132, and 8061). Data of OD_{595} represent the means of at least nine counts from three independent experiments. Error bars show standard deviations. (B) Biofilm formation capacity on polystyrene microtiter plates, quantification of the biofilm formed, and dot blot analysis of the PIA/PNAG accumulated by *S. aureus* MRSA strain 132 after 24 h hours of growth at 37°C in TSB-gluc and TSB-NaCl media. For dot blot analysis, a 1:25 and a 1:50 dilution of the samples were spotted onto nitrocellulose membranes, and PIA/PNAG production was detected with an anti-PIA/PNAG antiserum. OD_{595} data represent the means of at least nine counts from three independent experiments. Error bars show standard deviations.

was required for biofilm development in TSB-NaCl medium (Fig. 2A).

We next investigated the composition of the PIA/PNAG-independent biofilm matrix produced in TSB-gluc by means of dispersion experiments with proteinase K and sodium metaperiodate. The results showed that the glucose-induced biofilm was resistant to removal by sodium metaperiodate but sensitive to detachment by proteinase K, suggesting that a proteinaceous compound was responsible for the glucose-induced biofilm development (Fig. 2B). Taken together, these results allowed the selection of an *S. aureus* strain (132) that was able to form two types of biofilms: one that depended on PIA/PNAG production and was formed under TSB-NaCl (3%) growth conditions, and another one that was PIA/PNAG independent while requiring a proteinaceous compound and was produced under TSB-gluc incubating conditions.

Identification of the protein(s) mediating glucose-induced biofilm development. Based on previous results showing that different LPXTG proteins, such as Bap, SasG, and protein A, are able to mediate biofilm development in *S. aureus*, we first explored the possibility that a member of the LPXTG family of proteins was responsible for biofilm development in TSB-gluc. To test this hypothesis, we mutated the sortase A gene, required for the covalent anchoring of the LPXTG proteins to the cell wall, in strain 132. The resulting mutant completely lost the capacity to form a biofilm in TSB-gluc medium but retained the ability to form a biofilm in TSB-NaCl (Fig. 3A). These results suggested that at least one LPXTG protein was involved in the biofilm-forming capacity of strain 132 in TSB-gluc, whereas it had no role in PIA/PNAG-mediated biofilm development.

Analyses of the different *S. aureus* sequenced genomes showed that each isolate contains a unique repertoire of LPXTG proteins. Additionally, some specific proteins, such as Bap and Pls, have only been described in a few strains. In order to determine the set of LPXTG proteins present in MRSA strain 132, its corresponding genome was sequenced using the 454 technology. After that, we carried out the systematic mutation of each of the 20 LPXTG proteins encoding the identified genes. Thereby, *bap*, *cna*, *pls*, and *sasK* were not considered in the mutagenesis protocol, since they are not present in the genome of MRSA strain 132, and two putative LPXTG proteins (SA0927 and SA1888) were included in the assay (Table 1). Biofilm formation experiments of the resulting mutant strains in TSB-gluc medium revealed that only deletion of *fnbB* diminished the capacity of strain 132 to form a biofilm (Fig. 3B). Considering the sequence homology between *fnbB* and *fnbA*, we hypothesized that both proteins might be in-

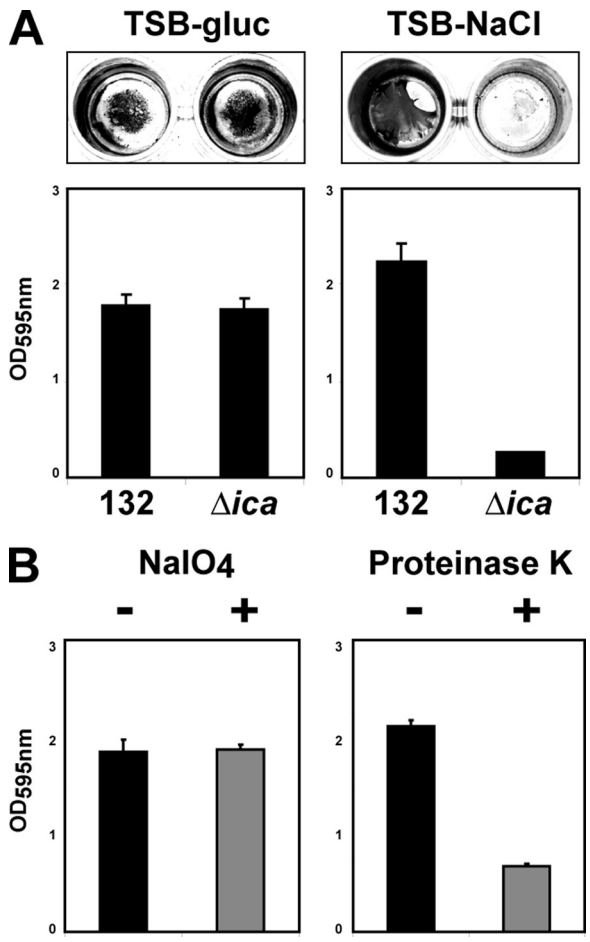

FIG. 2. Effect of Δ*icaADBC* deletion on the biofilm-forming capacity of MRSA strain 132 and phenotypic characterization of the PIA/PNAG-independent biofilm. (A) Biofilm formation of *S. aureus* strain 132 and its Δ*ica* mutant after having grown on microtiter plates for 24 h under static conditions at 37°C in TSB-gluc and TSB-NaCl media. To measure the biofilm formed, the amount of crystal violet-stained cells was quantified by solubilizing the dye in ethanol/acetone and determining the absorbance at 595 nm. Data represent the means of at least nine counts from three independent experiments. Error bars show standard deviations. (B) Detachment experiments. Biofilms formed by *S. aureus* strain 132 after having grown in TSB-gluc for 24 h were treated with sodium metaperiodate at 10 mM for 2 h at 37°C or with proteinase K at 100 μg/ml for 2 h at 37°C. The quantification of the nondetached biofilm was performed as described for panel A.

volved in the process and that compensatory effects might occur in single mutants. As a consequence, effects of the mutation of *fnbA* on biofilm formation would be veiled by the activity of FnBPB. To explore this hypothesis, a double Δ*fnbAB* mutant was constructed. Analysis of its biofilm formation capacity revealed that strain 132 Δ*fnbAB* completely lost the capacity to form a biofilm in TSB-gluc, indicating that in this media, both FnBPB and FnBPA cooperate to produce a biofilm (Fig. 4A). To exclude any role of PIA/PNAG exopolysaccharide in the production of biofilms by single *fnb* mutants, double Δ*ica* Δ*fnbA* and Δ*ica* Δ*fnbB* mutants as well as a triple Δ*ica* Δ*fnbAB* deletion mutant were constructed, and their biofilm-forming capacities were analyzed. The results demonstrated no role for PIA/PNAG production in the formation of the FnBP-mediated biofilm (Fig. 4A). We next investigated whether the specific requirement of FnBPs for biofilm development in TSB-gluc and of PIA/PNAG for biofilm development in TSB-NaCl correlated with higher *fnbB/ica* expression levels. For that, *fnbB* and *icaC* transcription levels in strain 132 grown in TSB-gluc and TSB-NaCl were determined by RT-PCR. In agreement with the observed phenotypes, the *fnbB* mRNA levels were significantly higher in cells grown in TSB-gluc than in cells grown in TSB-NaCl (Fig. 4D). In relation to *icaC*, despite the fact that strain 132 accumulates significantly higher levels of PIA/PNAG exopolysaccharide in TSB-NaCl (Fig. 1B), RT-PCR experiments did not reveal significant differences in *icaC* transcriptional levels when cells incubated in both media were analyzed (Fig. 4D), suggesting the existence of posttranscriptional regulatory mechanisms controlling PIA/PNAG synthesis.

Sequence analysis of the intergenic region between the *fnbA* and *fnbB* genes revealed the existence of a small open reading frame (ORF) (SACOL2510) encoding a protein of 40 amino acids of unknown function that is only present in some of the previously sequenced strains. To exclude the possibility that the deletion of this ORF during *fnbAB* allelic exchange could influence the biofilm-deficient phenotype displayed by the Δ*fnbAB* mutant, we performed a nonpolar deletion of this ORF. The resulting mutant 132 ΔSACOL2510 retained the capacity to form a biofilm in both TSB-gluc and TSB-NaCl (data not shown).

We further investigated the functionality of both FnBPA and FnBPB in biofilm development by complementation experiments. First, complementation of the double Δ*fnbAB* and triple Δ*ica* Δ*fnbAB* mutants with either *fnbA* or *fnbB* led to the production of a very thick and robust biofilm, indicating that both FnBPA and FnBPB are sufficient to promote biofilm development when individually overexpressed in the cells (Fig. 4B). Second, overexpression of either FnBPA or FnBPB in the wild-type strain 132 and other genetically unrelated *S. aureus* strains such as RN4220, G-6478, and 10833 also resulted in a significant induction/enhancement of the biofilm-forming capacity of these strains, demonstrating that promotion of biofilm development by FnBPs occurs irrespective of the genetic background (Fig. 4C). Overall, these results identified FnBPs, among all LPXTG proteins, as essential components of the biofilm formed by *S. aureus* strain 132 under TSB-gluc conditions.

FnBPs induce biofilm formation under continuous-flow conditions. We next investigated whether *S. aureus* strain 132 retained the capacity to switch between proteinaceous and exopolysaccharidic biofilm matrixes when grown under continuous-flow culture conditions in microfermenters. In agreement with previous results, visualization of both macroscopic biofilm development in microfermenters and biofilm cell density on removable glass slides showed that strain 132 Δ*fnbAB* lost the capacity to form a glucose-induced biofilm but retained the ability to produce a biofilm after 24 h of growth in TSB-NaCl. Conversely, a 132 Δ*ica* mutant lost only the capacity to form a NaCl-induced biofilm (Fig. 5A). Together, these results indicate that FnBPs are also able to promote cell-to-cell interactions and biofilm formation under continuous-flow conditions in TSB-gluc.

Next, we compared the architectures of the FnBP- and PIA/

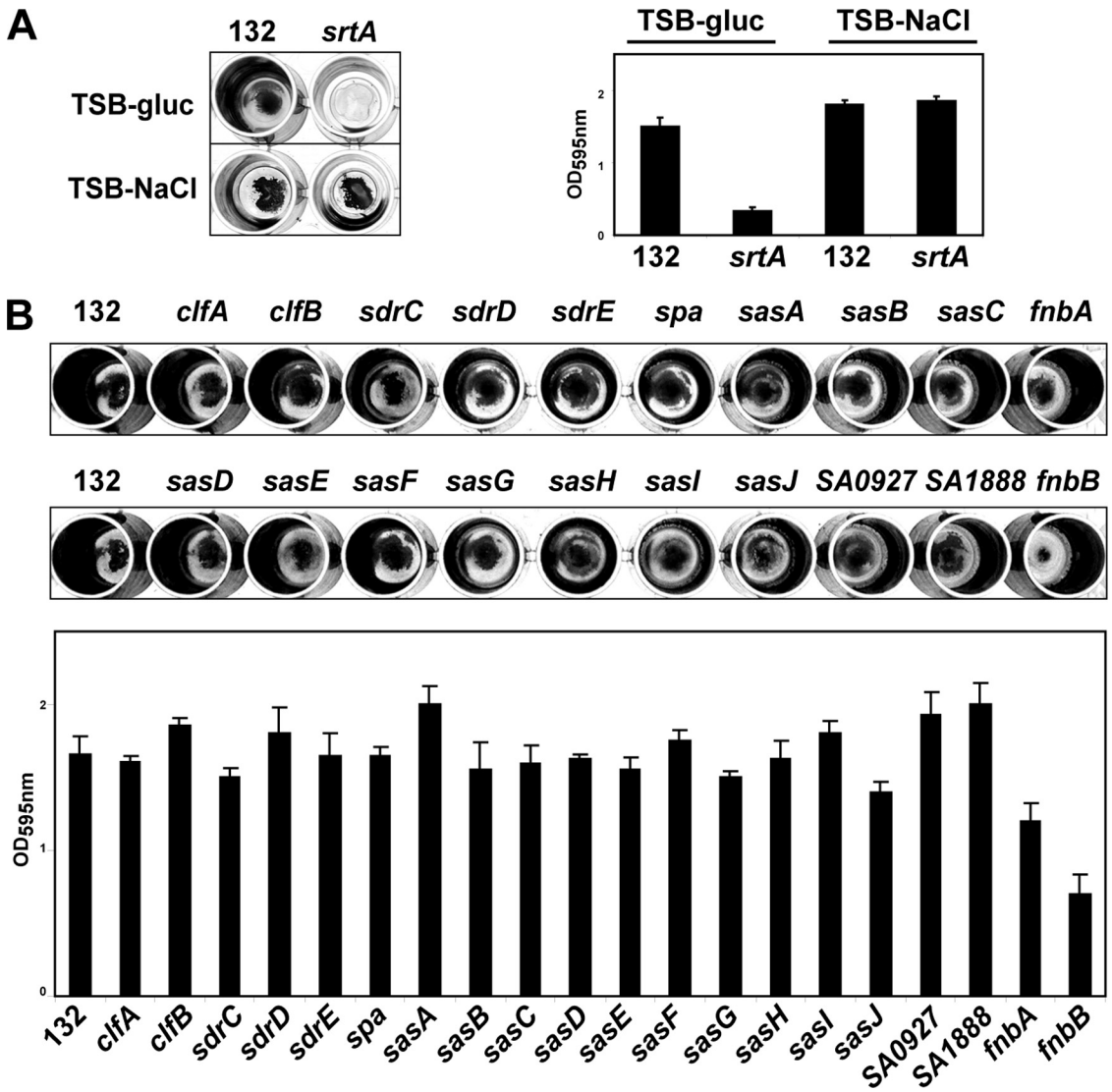

FIG. 3. Analyses of the contributions of the LPXTG proteins to the production of the proteinaceous biofilm formed by *S. aureus* strain 132. (A) Biofilm formation capacities of *S. aureus* strain 132 and its *srtA* mutant on microtiter polystyrene plates after 24 h of static incubation in TSB-gluc and TSB-NaCl media. (B) Biofilm formation capacities of *S. aureus* strain 132 and each LPXTG mutant on microtiter polystyrene plates after 24 h of static incubation in TSB-gluc medium. Representative pictures of at least three independent assays are shown. To measure the biofilm formed, the amount of crystal violet-stained cells was quantified by solubilizing the dye in ethanol/acetone and determining the absorbance at 595 nm. Data represent the means of at least nine counts from three independent experiments. Error bars show standard deviations.

PNAG-dependent biofilm matrixes by scanning electron microscopy. For that, biofilms developed in microfermenters by strain 132 Δ*ica* in TSB-gluc medium and strain 132 Δ*fnbAB* in TSB-NaCl medium were observed. The scanning electron micrographs revealed that cells growing in a FnBP-mediated biofilm form highly dense bacterial aggregates where a close contact between cells exists. The presence of extracellular matrix surrounding the bacteria or occupying the little void space between bacteria was undetectable (Fig. 5B). In the case of the PIA/PNAG-dependent biofilm, cells were embedded in an abundant extracellular matrix mesh that interconnected the bacteria (Fig. 5B).

Role of *agr* in the *S. aureus* strain 132 biofilm formation process. Sequence analysis of the *S. aureus* strain 132 genome revealed the existence of a single nucleotide deletion on *agrC* that causes a frameshift, which results in the premature inactivation of the protein. Since it has been shown that transcription of *fnb* genes is negatively regulated by *agr* (44, 56, 57), we decided to investigate the impact of such *agr* deficiency on the biofilm formation process of strain 132. For that, we complemented strain 132 with the pALC2073RNAIII plasmid that contains RNAIII under the control of a tetracycline-inducible promoter. Expression of RNAIII was confirmed by hemolytic activity on sheep blood agar plates (data not shown). We also generated a complete deletion of *agrBDCA* to exclude any effect of *agrA* on FnBP expression (40).

As shown in Fig. 6, expression of RNAIII in strain 132 reduced the FnBP levels and consequently its biofilm formation capacity in TSB-gluc, whereas it did not affect PIA/PNAG expression and biofilm formation in TSB-NaCl. Deletion of

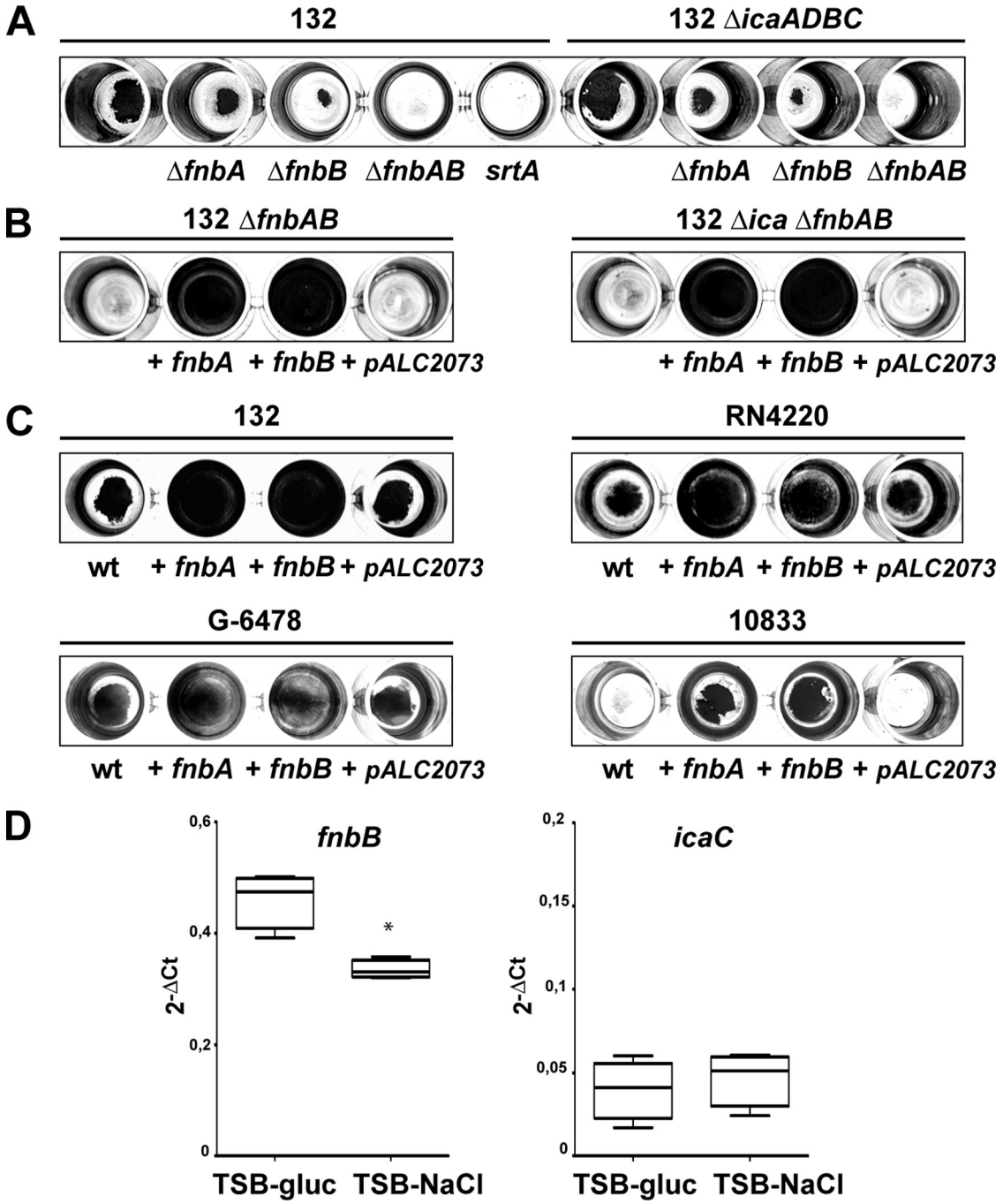

FIG. 4. FnBPA and FnBPB cooperate in the production of the biofilm formed in TSB-gluc. (A) Biofilm formation on microtiter polystyrene plates after 24 h of static incubation at 37°C, in TSB-gluc medium, of single and double mutants in FnBPs in strain 132 and a strain 132 Δ*ica* background. (B) Complementation experiments. Mutants 132 Δ*fnbAB* and 132 Δ*ica* Δ*fnbAB* were complemented with plasmid pFNBA4, which overexpresses the *fnbA* gene, plasmid pFNBB4, which overexpresses the *fnbB* gene, or plasmid pALC2073, as a control. (C) Overexpression experiments. Strains 132, RN4220, G-6478, and 10833 were transformed with plasmid pFNBA4, which overexpresses the *fnbA* gene, plasmid pFNBB4, which overexpresses the *fnbB* gene, or plasmid pALC2073, as a control. Biofilm formation capacity in microtiter plates was analyzed using TSB-gluc as a growth medium. Representative pictures of at least three independent assays are shown. wt, wild type. (D) RT-PCR analysis of *fnbB* (left side) and *icaC* (right side) mRNA levels in *S. aureus* strain 132 grown in TSB-gluc or TSB-NaCl at 37°C. The *gyrB* transcript was used as an endogenous control, and the results were expressed as the *n*-fold difference relative to the control gene ($2^{-\Delta Ct}$, where ΔCt represents the difference in threshold cycle between the target and control genes). Significant differences were detected when *fnbB* transcription in TSB-gluc and TSB-NaCl was compared (∗, $P < 0.05$; $n = 4$; Mann-Whitney test).

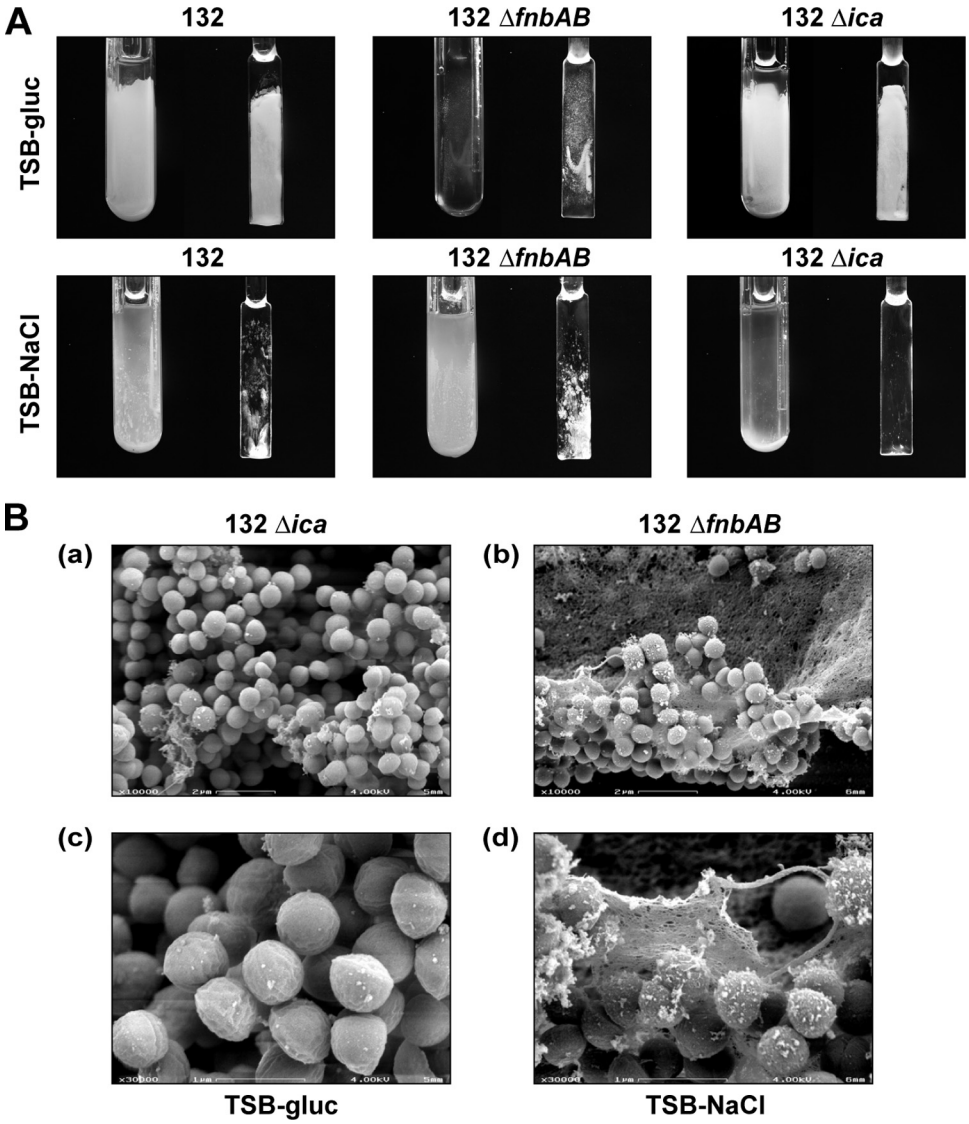

FIG. 5. Biofilm formation under continuous-flow conditions. (A) Biofilm development of wild-type *S. aureus* strain 132 and its Δ*fnbAB* and Δ*ica* mutants in microfermenters under continuous-flow conditions in TSB-gluc or TSB-NaCl media after 24 h at 37°C. The microfermenters contained the glass slides where bacteria formed the biofilms. The results of a representative experiment are shown. (B) Scanning electron microscopy analysis of the biofilms developed in microfermenters. Scanning electron micrographs of the *S. aureus* strain 132 Δ*ica* mutant grown in TSB-gluc medium (a, c) and the strain 132 Δ*fnbAB* mutant grown in TSB-NaCl medium (b, d) at ×10,000 (a, b) and ×30,000 (c, d) magnifications. Scale bars: a and b, 2 μm; c and d, 1 μm.

agrBDCA neither affected FnBP levels nor biofilm formation capacity compared to strain 132.

SOS response induces FnBP expression and biofilm formation. It has been described previously that LexA specifically binds to the *fnbB* promoter region, repressing gene transcription and thus protein expression until high or persistent DNA damage occurs (7). We wondered whether activation of the SOS response could enhance FnBP-mediated biofilm formation. To test this hypothesis, biofilm formation assays were performed on polystyrene plates in the presence of mitomycin C as a SOS response inductor. The biofilm formation capacities of the wild-type strain and Δ*fnbA* and Δ*ica* mutants increased when mitomycin C (0.05 μg/ml) was added to the growth medium (Fig. 7A). As expected, such induction was observed neither in the Δ*fnbB* nor in the Δ*fnbAB* mutant. To prove that the addition of mitomycin C correlated with increased FnBP expression, a Western ligand affinity blotting was performed in the presence of increasing concentrations of mitomycin C. As expected, mitomycin C induced accumulation of FnBPs in a concentration-dependent manner (Fig. 7B).

It is known that substitution of glutamate for glycine at the Ala-Gly LexA cleavage site results in a noncleavable repressor [LexA(G94E)] that is less sensitive to SOS induction (29). To confirm the role of LexA in the mitomycin C-mediated FnBP biofilm induction, we replaced the *lexA* coding sequence with the noncleavable *lexA* allele in the wild-type strain 132 and found that mitomycin C was not able to induce FnBP expression and biofilm formation in the resulting mutant (Fig. 7C).

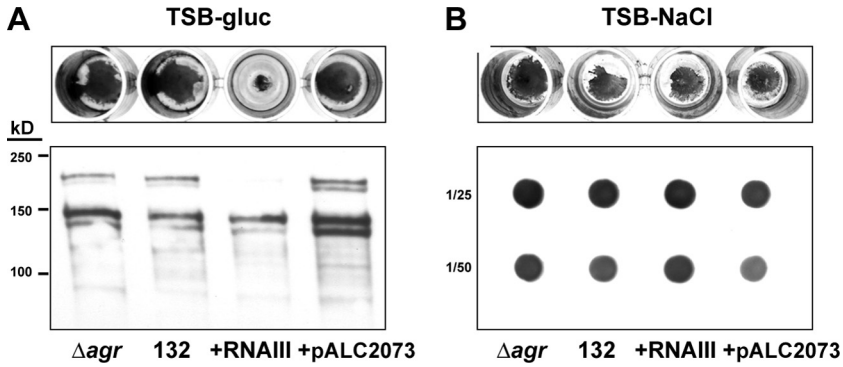

FIG. 6. Complementation with RNAIII reduces FnBP-mediated biofilm formation. (A) Biofilm formation on microtiter plates and FnBP levels of *S. aureus* strain 132, its Δ*agr* mutant, and strain 132 transformed with pALC2073RNAIII or pALC2073 empty plasmid after 24 h of static incubation at 37°C in TSB-gluc medium. Tetracycline was added at 125 ng/ml to plasmid-containing strains to facilitate induction (upper panel). Surface-associated protein extracts were analyzed by SDS-PAGE and detected by Western ligand affinity blotting using biotinylated human fibronectin as a ligand (bottom panel). (B) Biofilm formation on microtiter plates and PIA/PNAG levels of *S. aureus* strain 132, its Δ*agr* mutant, and strain 132 transformed with pALC2073RNAIII or pALC2073 empty plasmid after 24 h of static incubation at 37°C in TSB-gluc medium. Tetracycline was added at 125 ng/ml to plasmid-containing strains to facilitate induction (upper panel). For dot blot analysis, a 1:25 and a 1:50 dilution of the samples were spotted onto nitrocellulose membranes and PIA/PNAG production was detected with an anti-PIA/PNAG antiserum (bottom panel).

Together, these results demonstrate that an increase of FnBPB expression by activation of a LexA-dependent SOS response promotes the development of a FnBP-dependent biofilm.

FnBPs contribute to subcutaneous catheter infection. Considering the advantage that strain 132 is able to produce at least two types of biofilms that differ in their matrix nature, we investigated which one, the PIA/PNAG- or the FnBP-mediated biofilm, plays a more relevant role in vivo. To address this question, a murine subcutaneous catheter infection model was used. A total of 60 mice divided in groups of 10 were used in the experiment. Catheters were aseptically implanted in the subscapular spaces of the mice and coinfected with equal numbers of strain 132 and its corresponding *fnbAB* mutant, with strain 132 and its corresponding *ica* mutant, and with strain 132 and its double Δ*ica fnbAB* mutant. Bacteria were recovered

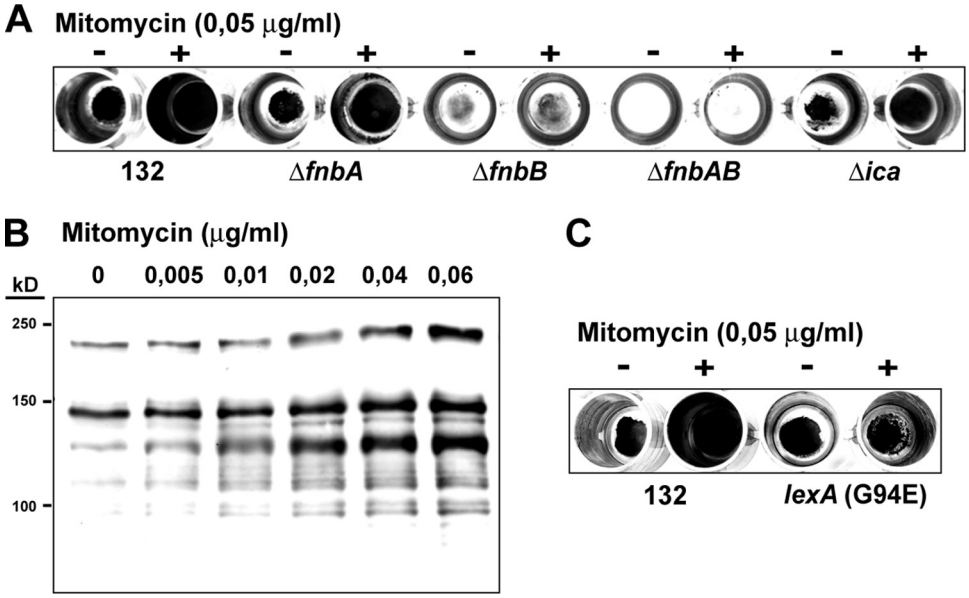

FIG. 7. The activation of a LexA-dependent SOS response induces FnBPB expression, resulting in a reinforcement of biofilm development. (A) Biofilm formation on microtiter plates of *S. aureus* strain 132 and its Δ*fnbA*, Δ*fnbB*, Δ*fnbAB*, and Δ*ica* mutants after 24 h of static incubation at 37°C in TSB-gluc medium supplemented with or without 0.05 μg/ml of mitomycin C. A representative picture of at least three independent assays is shown. (B) Detection of FnBP levels in the presence of increasing mitomycin C concentrations. Strain 132 surface-associated protein extracts prepared from cells grown for 4 h, in TSB-gluc medium supplemented with increasing mitomycin C concentrations, were analyzed by SDS-PAGE and detected by Western ligand affinity blotting using biotinylated human fibronectin as a ligand. (C) Biofilm formation on microtiter plates of *S. aureus* strain 132 and its *lexA*(G94E) mutant after 24 h of static incubation at 37°C in TSB-gluc medium supplemented with or without 0.05 μg/ml of mitomycin C. A representative picture of at least three independent assays is shown.

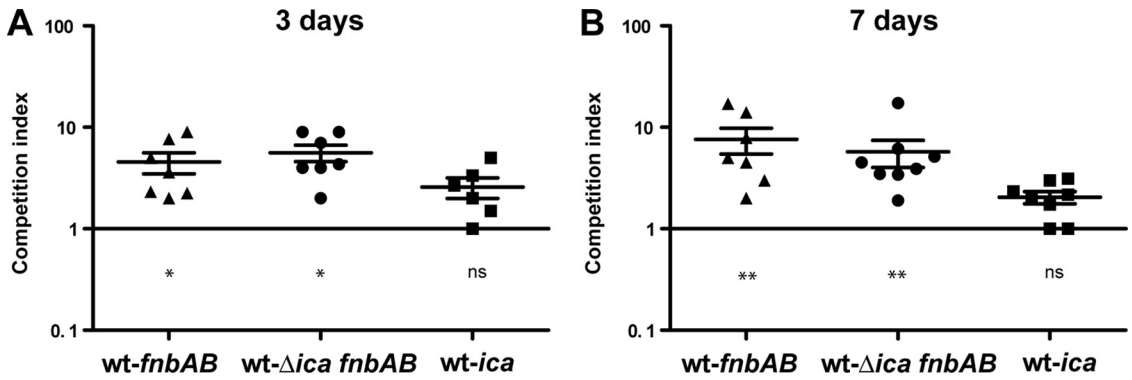

FIG. 8. Comparison of the contributions of a PIA/PNAG- and a FnBP-dependent biofilm to *S. aureus* virulence. Competition index of *fnbAB*, Δ*ica fnbAB*, and *ica* mutants tested against the wild-type (wt) 132 strain. Catheters were coinfected with equal numbers of the strains tested, and bacteria were recovered from implanted catheters and counted after 3 days (A) or 7 days (B) postinfection. Competition indexes were calculated and statistical differences were determined with the Wilcoxon's test. Horizontal bars represent the means of the competition indexes. Error bars represent standard errors of the means. Asterisks indicate that competition indexes are significantly greater than one (*, $P < 0.05$ [significant]; **, $P < 0.01$ [very significant]). ns, nonsignificant differences.

from implanted catheters at 3 or 7 days postinfection, and the number of bacteria was determined by a plate count as described in Materials and Methods. To evaluate and quantify the contribution of each strain tested to the infection, we used the competition index method. Using this technique, a competition index equal to 1 indicates similar virulence for both strains, a competition index significantly greater than 1 indicates a defect in virulence of the mutant strain, and a competition index significantly lower than 1 indicates the opposite. Prior to the start of the coinfection assays, a competition experiment was performed with all strains tested to confirm that strain growth was not affected by coincubation with others.

The results showed that after 3 days, both strain 132 *fnbAB* and strain 132 Δ*ica fnbAB* mutants showed a significant defect in catheter invasion in relation to the wild-type strain (Fig. 8A). This defect became very significant after 7 days postinfection (Fig. 8B). No significant differences were found when strain 132 *ica* and the wild-type strain were compared, at either 3 days or 7 days postinfection (Fig. 8).

Together, these results strongly suggest that in strain 132, FnBPs play a more relevant role than PIA/PNAG exopolysaccharide in the colonization of implanted devices.

DISCUSSION

One of the most unforeseen results revealed by the intense study of the *S. aureus* biofilm formation process during the last few years is the existence of surface proteins able to induce biofilm development in the absence of exopolysaccharides. The existence of alternative mechanisms to induce biofilm development implies that each *S. aureus* isolate might have specialized in the development of a particular type of biofilm matrix that would better suit the environment where it grows. Alternatively, different mechanisms might coexist in the same isolate, and thus, bacteria would make use of a particular one depending on specific environmental conditions. In support of the last hypothesis, a spontaneous switch to a proteinaceous biofilm matrix in a *Staphylococcus epidermidis ica*::IS*256* insertion mutant has recently been reported (20). In our study, we have identified and analyzed a clinical MRSA isolate able to switch between a polysaccharidic (PIA/PNAG) and a proteinaceous (FnBP) biofilm matrix depending on environmental conditions. The importance of this strain lies in the possibility of studying, on one hand, the specific properties that each biofilm matrix bestows on bacteria and, on the other hand, the signal transduction mechanisms involved in the modulation of the biofilm matrix composition according to specific environmental cues.

We made use of scanning electron microscopy to compare the structures of the FnBP- and PIA/PNAG exopolysaccharide-dependent biofilm matrixes. The results revealed that cells growing in a FnBP-mediated biofilm were closely attached without detectable extracellular matrix surrounding the bacteria. In contrast, PIA/PNAG-dependent biofilms showed abundant extracellular material in which bacteria were embedded. Thus, the FnBP-dependent multicellular behavior does not fit, sensu stricto, into the conventional biofilm definition of "a microbially derived sessile community characterized by cells that are irreversibly attached to a substratum or interface or to each other and embedded in a matrix of extracellular polymeric substances that they have produced" (12). Taking this into account, and considering that scanning microscopy analysis of a Bap-mediated biofilm showed similar tightly attached bacteria (our unpublished results), we propose that a protein-mediated biofilm should be referred to as "multicellular behavior."

The versatility of the elements responsible for *S. aureus* multicellular behavior is not restricted to the simple option between a polysaccharidic or a proteinaceous component. *S. aureus* cells can opt for at least four different surface proteins, Bap, SasG, protein A, and FnBPs, to achieve protein-mediated multicellular behavior (9, 11, 27, 33, 36, 46). Thus, the question arises of whether the properties that the community lifestyle confers to bacteria differ depending on the protein that promotes cell-to-cell interactions. In the case of strain 132, we performed the systematic disruption of the 20 genes encoding LPXTG proteins present in its genome to find out the protein(s) involved in the production of a protein-mediated biofilm formed under TSB-gluc conditions. Analysis of every mu-

tant revealed that only the absence of FnBPs inhibited the capacity of strain 132 to produce multicellular communities in that medium. Thus, in the case of this particular strain and under TSB-gluc environmental conditions, neither SasG nor protein A seems to play any role in multicellular behavior. This situation might simply be due to compensatory effects between other proteins that would mask the effect of the single mutants. Alternatively, it is likely that the laboratory conditions used in our study might not be appropriate for inducing SasG or protein A expression to the levels required to induce a macroscopically noticeable multicellular behavior. In support of this assumption, our results confirmed a direct relationship between the FnBP expression levels and the strength of the multicellular phenotype. First, overexpression of FnBPs in wild-type strains induced multicellular behavior. Second, the enhanced FnBP accumulation due to the spontaneous *agr* mutation promoted multicellular behavior. Third, induction of FnBPB expression through activation of the SOS response significantly increased the number of bacteria taking part of the multicellular community. In this regard, regulation of FnBPB expression by the SOS response has been previously determined (7). In their study, Bisognano et al. showed that LexA is a repressor of *fnbB* expression, and consequently, SOS response induction by commonly used fluoroquinolones resulted in the increased expression of the FnBPB protein on the bacterial surface (7). As FnBPs have been shown to play an important role during invasion of mammalian cells (47, 48) and in mediating adherence to different host extracellular matrix components, such as fibronectin, fibrinogen, elastin, or tropoelastin (23, 43, 55), an adverse consequence of SOS induction by antibiotics would be that it might facilitate colonization of host cells and medical implants (13, 17). Accordingly, our results suggest that an increase in FnBPB expression through activation of the SOS response is sufficient to induce a noticeable increase in the capacity of the strain to produce multicellular communities on abiotic surfaces in vitro.

It has recently been shown that spontaneous *agr* mutants frequently arise in vivo during the course of the infection (51). Although the benefits that *agr* genotypic instability might provide to *S. aureus* in human infection remain unknown, different studies have shown that *agr* mutants have a tendency to form biofilms in vitro. Enhanced biofilm formation by *agr* mutants has been attributed to (i) decreased production of RNAIII-encoded δ-toxin, which has surfactant properties (54), (ii) decreased production of extracellular proteases, which can digest the proteinaceous biofilm matrix (8), and (iii) increased accumulation of protein A that promotes aggregation and cell-to-cell interactions (33). In addition to these mechanisms, our results indicate that the increased accumulation of FnBPs accounts for another mechanism through which *agr* mutation can contribute to biofilm development. A previous study investigating the role of *agr* in clinical *S. aureus* MRSA isolates reported that inactivation of *agr* increased *ica*-independent biofilm development in 5 out of the 13 isolates investigated (37). However, it is likely that this study underestimated the implication of *agr* since some of these isolates might already be natural *agr* mutants and consequently complementation with RNAIII would be needed to determine the effects of *agr* on biofilm development. Afterward, the same group demonstrated that FnBPs were responsible for promoting biofilm development in five genetically unrelated MRSA isolates (36). These results suggest that MRSA isolates, like the one used in this study, with the capacity to switch between a FnBP- and a PIA/PNAG-based biofilm might frequently occur in clinical settings.

To address the biological significance of PIA/PNAG and FnBPs during colonization of implanted devices by strain 132, we compared the capacities of the wild-type strain and the isogenic *fnbAB*, *ica*, and Δ*ica fnbAB* mutants to colonize an implanted catheter by using a murine foreign-body infection model. We found that the absence of FnBPs caused a significant reduction in the capacity of the strain to colonize catheters in vivo after 3 and 7 days postinfection. In contrast, the absence of the *icaADBC* operon did not lead to any significant reduction. It is important to note that in our experimental model, attachment of *S. aureus* to native implants occurred because catheters were immediately infected after implantation without making use of a precoating period with plasma proteins such as fibronectin. The role of PIA/PNAG exopolysaccharide during the infection process has been addressed in various studies with contradictory outcomes. Thus, PIA/PNAG production has been described as essential for virulence in murine models of systemic infection while deletion of the *ica* locus failed to alter virulence in device-related infection models (15, 16, 25, 26). Our results are in agreement with a previous study focused on the analysis of the role of SarA in biofilm development in vivo. In this study, Beenken et al. found that an *S. aureus* UAMS-1 *sarA* mutant presented a reduced capacity to colonize catheters in vivo whereas the UAMS-1 *ica* mutant colonized the catheters as efficiently as the wild-type strain using a murine model in which catheters were infected 1 h after implantation (6). Interestingly, biofilm formation in the UAMS-1 isolate was enhanced by coating the substrate with plasma proteins and was not dependent on PIA/PNAG production (5, 6). Based on these data, and taking into account that expression of FnBPs is completely abolished in the absence of *sarA* (36, 46), it is tempting to speculate that the UAMS-1 strain might produce a FnBP-dependent biofilm whose expression would be completely abolished in the *sarA* mutant strain. Thus, a reduced recovery of the *sarA* mutant in coinfection experiments with implanted catheters might be due to FnBP deficiency (6).

An association between methicillin resistance and protein-dependent multicellular behavior in *S. aureus* has been postulated (14, 36, 37). If such an association exists, elucidation of the properties that FnBPs confer to the bacterial community during the colonization of implanted medical biomaterials may contribute to our understanding of the factors that play a role in the persistence and transmission of MRSA isolates across the hospitals of developed countries.

ACKNOWLEDGMENTS

Marta Vergara-Irigaray is a predoctoral fellow (FPU) from the Ministerio de Educacióon y Ciencia, Spain. Jaione Valle and Alejandro Toledo-Arana have JAE-Doc research contracts from CSIC.

We thank T. Maira-Litrán and J. Pier, Harvard Medical School of Boston, for providing us the anti-PIA/PNAG antiserum; A. L. Cheung, Dartmouth Medical School of Hanover, for the pALC2073 plasmid; and Jérôme Etienne, Centre National de Référence des Staphylocoques of Lyon, France, and the Microbiology Department of Clínica

Universitaria de Navarra, Spain, for providing the *S. aureus* isolates analyzed in this article.

This work was supported by the BIO2005-08399 and ERA-NET Pathogenomics (GEN2006-27792-C2-1-E/PAT) grants from the Spanish Ministerio de Ciencia, the Euroinnova Navarra-INNOVATIC program from the Gobierno de Navarra, and the Staph Dynamics LSHM-CT-2006-019064 grant from the European Union.

REFERENCES

1. **Arnaud, M., A. Chastanet, and M. Débarbouillé.** 2004. New vector for efficient allelic replacement in naturally nontransformable, low-GC-content, gram-positive bacteria. Appl. Environ. Microbiol. **70:**6887–6891.
2. **Arrizubieta, M. J., A. Toledo-Arana, B. Amorena, J. R. Penades, and I. Lasa.** 2004. Calcium inhibits Bap-dependent multicellular behavior in *Staphylococcus aureus*. J. Bacteriol. **186:**7490–7498.
3. **Ausubel, F. M., R. Brent, R. E. Kingston, D. D. Moore, J. G. Seidman, J. A. Smith, and K. Struhl (ed.).** 1990. Current protocols in molecular biology. John Wiley & Sons, New York, NY.
4. **Bateman, B. T., N. P. Donegan, T. M. Jarry, M. Palma, and A. L. Cheung.** 2001. Evaluation of a tetracycline-inducible promoter in *Staphylococcus aureus* in vitro and in vivo and its application in demonstrating the role of *sigB* in microcolony formation. Infect. Immun. **69:**7851–7857.
5. **Beenken, K. E., J. S. Blevins, and M. S. Smeltzer.** 2003. Mutation of *sarA* in *Staphylococcus aureus* limits biofilm formation. Infect. Immun. **71:**4206–4211.
6. **Beenken, K. E., P. M. Dunman, F. McAleese, D. Macapagal, E. Murphy, S. J. Projan, J. S. Blevins, and M. S. Smeltzer.** 2004. Global gene expression in *Staphylococcus aureus* biofilms. J. Bacteriol. **186:**4665–4684.
7. **Bisognano, C., W. L. Kelley, T. Estoppey, P. Francois, J. Schrenzel, D. Li, D. P. Lew, D. C. Hooper, A. L. Cheung, and P. Vaudaux.** 2004. A recA-LexA-dependent pathway mediates ciprofloxacin-induced fibronectin binding in *Staphylococcus aureus*. J. Biol. Chem. **279:**9064–9071.
8. **Boles, B. R., and A. R. Horswill.** 2008. Agr-mediated dispersal of *Staphylococcus aureus* biofilms. PLoS Pathog. **4:**e1000052.
9. **Corrigan, R. M., D. Rigby, P. Handley, and T. J. Foster.** 2007. The role of *Staphylococcus aureus* surface protein SasG in adherence and biofilm formation. Microbiology **153:**2435–2446.
10. **Cramton, S. E., C. Gerke, N. F. Schnell, W. W. Nichols, and F. Gotz.** 1999. The intercellular adhesion (*ica*) locus is present in *Staphylococcus aureus* and is required for biofilm formation. Infect. Immun. **67:**5427–5433.
11. **Cucarella, C., C. Solano, J. Valle, B. Amorena, I. Lasa, and J. R. Penades.** 2001. Bap, a *Staphylococcus aureus* surface protein involved in biofilm formation. J. Bacteriol. **183:**2888–2896.
12. **Donlan, R. M., and J. W. Costerton.** 2002. Biofilms: survival mechanisms of clinically relevant microorganisms. Clin. Microbiol. Rev. **15:**167–193.
13. **Fischer, B., P. Vaudaux, M. Magnin, Y. el Mestikawy, R. A. Proctor, D. P. Lew, and H. Vasey.** 1996. Novel animal model for studying the molecular mechanisms of bacterial adhesion to bone-implanted metallic devices: role of fibronectin in *Staphylococcus aureus* adhesion. J. Orthop. Res. **14:**914–920.
14. **Fitzpatrick, F., H. Humphreys, and J. P. O'Gara.** 2005. Evidence for *icaADBC*-independent biofilm development mechanism in methicillin-resistant *Staphylococcus aureus* clinical isolates. J. Clin. Microbiol. **43:**1973–1976.
15. **Fluckiger, U., M. Ulrich, A. Steinhuber, G. Doring, D. Mack, R. Landmann, C. Goerke, and C. Wolz.** 2005. Biofilm formation, *icaADBC* transcription, and polysaccharide intercellular adhesin synthesis by staphylococci in a device-related infection model. Infect. Immun. **73:**1811–1819.
16. **Francois, P., P. H. Tu Quoc, C. Bisognano, W. L. Kelley, D. P. Lew, J. Schrenzel, S. E. Cramton, F. Gotz, and P. Vaudaux.** 2003. Lack of biofilm contribution to bacterial colonisation in an experimental model of foreign body infection by *Staphylococcus aureus* and *Staphylococcus epidermidis*. FEMS Immunol. Med. Microbiol. **35:**135–140.
17. **Greene, C., D. McDevitt, P. Francois, P. E. Vaudaux, D. P. Lew, and T. J. Foster.** 1995. Adhesion properties of mutants of *Staphylococcus aureus* defective in fibronectin-binding proteins and studies on the expression of *fnb* genes. Mol. Microbiol. **17:**1143–1152.
18. **Heilmann, C., C. Gerke, F. Perdreau-Remington, and F. Gotz.** 1996. Characterization of Tn*917* insertion mutants of *Staphylococcus epidermidis* affected in biofilm formation. Infect. Immun. **64:**277–282.
19. **Heilmann, C., O. Schweitzer, C. Gerke, N. Vanittanakom, D. Mack, and F. Gotz.** 1996. Molecular basis of intercellular adhesion in the biofilm-forming *Staphylococcus epidermidis*. Mol. Microbiol. **20:**1083–1091.
20. **Hennig, S., S. Nyunt Wai, and W. Ziebuhr.** 2007. Spontaneous switch to PIA-independent biofilm formation in an *ica*-positive *Staphylococcus epidermidis* isolate. Int. J. Med. Microbiol. **297:**117–122.
21. **Herman, R. A., V. R. Kee, K. G. Moores, and M. B. Ross.** 2008. Etiology and treatment of community-associated methicillin-resistant *Staphylococcus aureus*. Am. J. Health Syst. Pharm. **65:**219–225.
22. **Kaplan, J. B., K. Velliyagounder, C. Ragunath, H. Rohde, D. Mack, J. K. Knobloch, and N. Ramasubbu.** 2004. Genes involved in the synthesis and degradation of matrix polysaccharide in *Actinobacillus actinomycetemcomitans* and *Actinobacillus pleuropneumoniae* biofilms. J. Bacteriol. **186:**8213–8220.
23. **Keane, F. M., A. W. Clarke, T. J. Foster, and A. S. Weiss.** 2007. The N-terminal A domain of *Staphylococcus aureus* fibronectin-binding protein A binds to tropoelastin. Biochemistry **46:**7226–7232.
24. **Kennedy, A. D., M. Otto, K. R. Braughton, A. R. Whitney, L. Chen, B. Mathema, J. R. Mediavilla, K. A. Byrne, L. D. Parkins, F. C. Tenover, B. N. Kreiswirth, J. M. Musser, and F. R. Deleo.** 2008. Epidemic community-associated methicillin-resistant *Staphylococcus aureus*: recent clonal expansion and diversification. Proc. Natl. Acad. Sci. USA **105:**1327–1332.
25. **Kristian, S. A., T. Golda, F. Ferracin, S. E. Cramton, B. Neumeister, A. Peschel, F. Gotz, and R. Landmann.** 2004. The ability of biofilm formation does not influence virulence of *Staphylococcus aureus* and host response in a mouse tissue cage infection model. Microb. Pathog. **36:**237–245.
26. **Kropec, A., T. Maira-Litran, K. K. Jefferson, M. Grout, S. E. Cramton, F. Gotz, D. A. Goldmann, and G. B. Pier.** 2005. Poly-N-acetylglucosamine production in *Staphylococcus aureus* is essential for virulence in murine models of systemic infection. Infect. Immun. **73:**6868–6876.
27. **Kuroda, M., R. Ito, Y. Tanaka, M. Yao, K. Matoba, S. Saito, I. Tanaka, and T. Ohta.** 2008. *Staphylococcus aureus* surface protein SasG contributes to intercellular autoaggregation of *Staphylococcus aureus*. Biochem. Biophys. Res. Commun. **377:**1102–1106.
28. **Lim, Y., M. Jana, T. T. Luong, and C. Y. Lee.** 2004. Control of glucose- and NaCl-induced biofilm formation by *rbf* in *Staphylococcus aureus*. J. Bacteriol. **186:**722–729.
29. **Little, J. W.** 1993. LexA cleavage and other self-processing reactions. J. Bacteriol. **175:**4943–4950.
30. **Maira-Litran, T., A. Kropec, D. A. Goldmann, and G. B. Pier.** 2005. Comparative opsonic and protective activities of *Staphylococcus aureus* conjugate vaccines containing native or deacetylated staphylococcal poly-*N*-acetyl-β-(1-6)-glucosamine. Infect. Immun. **73:**6752–6762.
31. **Mazmanian, S. K., G. Liu, E. R. Jensen, E. Lenoy, and O. Schneewind.** 2000. *Staphylococcus aureus* sortase mutants defective in the display of surface proteins and in the pathogenesis of animal infections. Proc. Natl. Acad. Sci. USA **97:**5510–5515.
32. **Mckenney, D., K. Pouliot, V. Wang, V. Murthy, M. Ulrich, G. Döring, J. C. Lee, D. A. Goldmann, and G. B. Pier.** 1999. Broadly protective vaccine for *Staphylococcus aureus* based on an in vivo-expressed antigen. Science **284:**1523–1527.
33. **Merino, N., A. Toledo-Arana, M. Vergara-Irigaray, J. Valle, C. Solano, E. Calvo, J. A. Lopez, T. J. Foster, J. R. Penades, and I. Lasa.** 2009. Protein A-mediated multicellular behavior in *Staphylococcus aureus*. J. Bacteriol. **191:**832–843.
34. **Novick, R. P.** 1991. Genetic systems in staphylococci. Methods Enzymol. **204:**587–636.
35. **Novick, R. P.** 1990. The *Staphylococcus* as a molecular genetic system, p. 1–37. *In* R. P. Novick (ed.), Molecular biology of the *Staphylococcus*. VCH Publishers, New York, NY.
36. **O'Neill, E., C. Pozzi, P. Houston, H. Humphreys, D. A. Robinson, A. Loughman, T. J. Foster, and J. P. O'Gara.** 2008. A novel *Staphylococcus aureus* biofilm phenotype mediated by the fibronectin-binding proteins, FnBPA and FnBPB. J. Bacteriol. **190:**3835–3850.
37. **O'Neill, E., C. Pozzi, P. Houston, D. Smyth, H. Humphreys, D. A. Robinson, and J. P. O'Gara.** 2007. Association between methicillin susceptibility and biofilm regulation in *Staphylococcus aureus* isolates from device-related infections. J. Clin. Microbiol. **45:**1379–1388.
38. **Pattee, P. A.** 1981. Distribution of Tn*551* insertion sites responsible for auxotrophy on the *Staphylococcus aureus* chromosome. J. Bacteriol. **145:**479–488.
39. **Prigent-Combaret, C., G. Prensier, T. T. Le Thi, O. Vidal, P. Lejeune, and C. Dorel.** 2000. Developmental pathway for biofilm formation in curli-producing *Escherichia coli* strains: role of flagella, curli and colanic acid. Environ. Microbiol. **2:**450–464.
40. **Queck, S. Y., M. Jameson-Lee, A. E. Villaruz, T. H. Bach, B. A. Khan, D. E. Sturdevant, S. M. Ricklefs, M. Li, and M. Otto.** 2008. RNAIII-independent target gene control by the *agr* quorum-sensing system: insight into the evolution of virulence regulation in *Staphylococcus aureus*. Mol. Cell **32:**150–158.
41. **Rachid, S., S. Cho, K. Ohlsen, J. Hacker, and W. Ziebuhr.** 2000. Induction of *Staphylococcus epidermidis* biofilm formation by environmental factors: the possible involvement of the alternative transcription factor *sigB*. Adv. Exp. Med. Biol. **485:**159–166.
42. **Rachid, S., K. Ohlsen, W. Witte, J. Hacker, and W. Ziebuhr.** 2000. Effect of subinhibitory antibiotic concentrations on polysaccharide intercellular adhesin expression in biofilm-forming *Staphylococcus epidermidis*. Antimicrob. Agents Chemother. **44:**3357–3363.
43. **Roche, F. M., R. Downer, F. Keane, P. Speziale, P. W. Park, and T. J. Foster.** 2004. The N-terminal A domain of fibronectin-binding proteins A and B promotes adhesion of *Staphylococcus aureus* to elastin. J. Biol. Chem. **279:**38433–38440.
44. **Saravia-Otten, P., H. P. Muller, and S. Arvidson.** 1997. Transcription of *Staphylococcus aureus* fibronectin binding protein genes is negatively regulated by *agr* and an *agr*-independent mechanism. J. Bacteriol. **179:**5259–5263.

45. **Shanks, R. M., N. P. Donegan, M. L. Graber, S. E. Buckingham, M. E. Zegans, A. L. Cheung, and G. A. O'Toole.** 2005. Heparin stimulates *Staphylococcus aureus* biofilm formation. Infect. Immun. **73:**4596–4606.
46. **Shanks, R. M. Q., M. A. Meehl, K. M. Brothers, R. M. Martinez, N. P. Donegan, M. L. Graber, A. L. Cheung, and G. A. O'Toole.** 2008. Genetic evidence for an alternative citrate-dependent biofilm formation pathway of *Staphylococcus aureus* that is dependent on fibronectin binding proteins and the GraRS two-component regulatory system. Infect. Immun. **76:**2469–2477.
47. **Sinha, B., P. Francois, Y. A. Que, M. Hussain, C. Heilmann, P. Moreillon, D. Lew, K. H. Krause, G. Peters, and M. Herrmann.** 2000. Heterologously expressed *Staphylococcus aureus* fibronectin-binding proteins are sufficient for invasion of host cells. Infect. Immun. **68:**6871–6878.
48. **Sinha, B., P. P. Francois, O. Nusse, M. Foti, O. M. Hartford, P. Vaudaux, T. J. Foster, D. P. Lew, M. Herrmann, and K. H. Krause.** 1999. Fibronectin-binding protein acts as *Staphylococcus aureus* invasin via fibronectin bridging to integrin alpha5beta1. Cell Microbiol. **1:**101–117.
49. **Toledo-Arana, A., N. Merino, M. Vergara-Irigaray, M. Debarbouille, J. R. Penades, and I. Lasa.** 2005. *Staphylococcus aureus* develops an alternative, *ica*-independent biofilm in the absence of the *arlRS* two-component system. J. Bacteriol. **187:**5318–5329.
50. **Tormo, M. A., E. Knecht, F. Gotz, I. Lasa, and J. R. Penades.** 2005. Bap-dependent biofilm formation by pathogenic species of *Staphylococcus*: evidence of horizontal gene transfer? Microbiology **151:**2465–2475.
51. **Traber, K. E., E. Lee, S. Benson, R. Corrigan, M. Cantera, B. Shopsin, and R. P. Novick.** 2008. *agr* function in clinical *Staphylococcus aureus* isolates. Microbiology **154:**2265–2274.
52. **Ubeda, C., E. Maiques, E. Knecht, I. Lasa, R. P. Novick, and J. R. Penades.** 2005. Antibiotic-induced SOS response promotes horizontal dissemination of pathogenicity island-encoded virulence factors in staphylococci. Mol. Microbiol. **56:**836–844.
53. **Valle, J., A. Toledo-Arana, C. Berasain, J. M. Ghigo, B. Amorena, J. R. Penades, and I. Lasa.** 2003. SarA and not σ^B is essential for biofilm development by *Staphylococcus aureus*. Mol. Microbiol. **48:**1075–1087.
54. **Vuong, C., H. L. Saenz, F. Gotz, and M. Otto.** 2000. Impact of the *agr* quorum-sensing system on adherence to polystyrene in *Staphylococcus aureus*. J. Infect. Dis. **182:**1688–1693.
55. **Wann, E. R., S. Gurusiddappa, and M. Hook.** 2000. The fibronectin-binding MSCRAMM FnbpA of *Staphylococcus aureus* is a bifunctional protein that also binds to fibrinogen. J. Biol. Chem. **275:**13863–13871.
56. **Wolz, C., P. Pohlmann-Dietze, A. Steinhuber, Y. T. Chien, A. Manna, W. van Wamel, and A. Cheung.** 2000. Agr-independent regulation of fibronectin-binding protein(s) by the regulatory locus *sar* in *Staphylococcus aureus*. Mol. Microbiol. **36:**230–243.
57. **Xiong, Y. Q., A. S. Bayer, M. R. Yeaman, W. Van Wamel, A. C. Manna, and A. L. Cheung.** 2004. Impacts of *sarA* and *agr* in *Staphylococcus aureus* strain Newman on fibronectin-binding protein A gene expression and fibronectin adherence capacity in vitro and in experimental infective endocarditis. Infect. Immun. **72:**1832–1836.

Editor: J. B. Bliska